JCTC Journal of Chemical Theory and Computation

Article

pubs.acs.org/JCTC

Combining 2d-Periodic Quantum Chemistry with Molecular Force Fields: A Novel QM/MM Procedure for the Treatment of Solid-State Surfaces and Interfaces

Thomas S. Hofer* and Andreas O. Tirler

Theoretical Chemistry Division, Institute for General Inorganic and Theoretical Chemistry, Center for Chemistry and Biomedicine, University of Innsbruck, Innrain 80-82, A-6020 Innsbruck, Austria

Supporting Information

ABSTRACT: The feasibility of a novel approach for the hybrid quantum mechanical/molecular mechanical (QM/MM) treatment of solid-state surfaces without the requirement of artificially keeping atoms at fixed positions is explored. In order to avoid potential artifacts of the QM/MM transition near the surface, a 2d-periodic QM treatment of the system is employed. Thus, the only QM/MM interface between atoms of the solid is along the non-periodic z-dimension. It is shown for the metal oxide and metal systems MgO(100) and Be(0001) that a properly adjusted embedding potential supplemented by adequate non-Coulombic potentials (if required) enables the application of the QM/MM framework in all-atom structure optimization and molecular dynamics (MD) simulation. The commonly employed constraint to keep at least some of the embedding atoms at fixed position is not required. Two exemplary applications of H_2O on MgO(100) and H_2 on Be(0001) demonstrate the applicability of the framework in exemplary MD simulation studies.

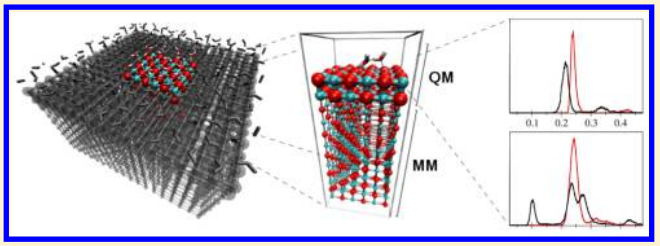

1. INTRODUCTION

With the invention of the transistor in 1947[1] the foundation for the development of microprocessor technology was laid, leading to countless innovations in science and engineering and sparking the advent of modern scientific computing. The impact of computational methods on numerous disciplines ranging from engineering and social sciences to physics and chemistry becomes more and more visible each year, and the awarding of the Nobel prize in Chemistry 2013 to Martin Karplus, Michael Levitt, and Arieh Warshel "for the development of multiscale models for complex chemical systems"[2] is a prominent example of this development. Among numerous contributions to the field of theoretical and computational chemistry the work of the Nobel laureates was termed "ground-breaking in that they managed to make Newtons classical physics work side-by-side with the fundamentally different quantum physics".[2]

The combination of these two theories was achieved by the formulation of so-called hybrid quantum mechanical/molecular mechanical (QM/MM) techniques,[3−7] initially developed for investigations of biomolecular systems. A key element of these simulation techniques is the separation of the chemical system into two subregions: The chemically most relevant part of the system is treated with accurate but time-consuming quantum mechanical (QM) techniques[8−11] describing the distribution of the electron density surrounding the nuclei. These methods employ numerical solutions of Schrödinger's equation[12] to obtain a quantitative description of the electronic structure, thereby taking important contributions such as polarization, charge-transfer, and many-body interactions into account. As no empirical parameters are required, these approaches are very general and enable first principle descriptions of virtually all classes of chemical systems. Due to their complexity the computational effort increases exponentially with system size, and, therefore, the number of atoms has to be reduced to a critical minimum in purely quantum mechanical investigations.

For this reason less time-consuming yet less accurate molecular mechanical (MM) methods[13−15] are considered sufficient to represent the interactions within the remaining part of the system. These empirical approaches also referred to as force fields (FF) treat the atomic interactions based on preparametrized potential functions, the respective accuracy and computational effort being strongly dependent on the considered interaction types (e.g. bonding, nonbonding, polarization, many-body effects, etc.) and the associated functional form. The development and balancing of a reliable parameter set for chemical systems is a challenging, tedious, and time-consuming task. Typically, force fields are focused on a particular class of molecules such as minerals,[16] ionic liquids,[17−19] or nucleic acids and peptides.[20−26] In practice limitations in the applicability, accuracy, and transferability may arise from the empirical character of MM approaches, for instance when two independent force field models are to be combined as it may be the case when studying solid interfaces.

A further severe limitation of MM approaches results from the harmonic approximation sketched in Figure 1: The majority of

Received: June 11, 2015
Published: October 28, 2015

DOI: 10.1021/acs.jctc.5b00548
J. Chem. Theory Comput. 2015, 11, 5873−5887

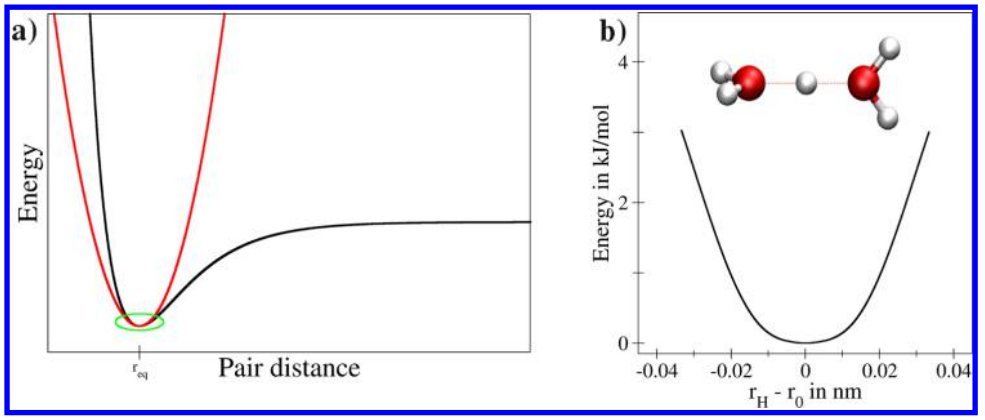

Figure 1. a) The majority of force fields model chemical bonds (black) via a harmonic approximation (red), which is only valid close to the equilibrium distance r_{eq} (green region). Cleavage and formation of the bond cannot be described. b) Reaction coordinate of the proton transfer in the $H_5O_2^+$ system described at quantum mechanical level (DFT PBE functional).

force fields model intramolecular bonds via a spring-like interaction,[13−15] which prevents the description of the formation and cleavage of chemical bonds. Although the development of reactive force fields enabling topology changes in the course of a simulation enjoyed increased interest in the past decade,[27−41] results obtained from first-principles provide a fundamental source of data for the parametrization and assessment of such advanced MM methods.

Thus, the strength of a QM/MM treatment lies in the combination of the accuracy and capabilities of QM approaches (i.e., the description of chemical reactions) with the efficiency of simple MM methods to model the respective environment. Various formulations of the QM/MM technique have enjoyed widespread application and success during the last decades[42−46] not only in the context of biomolecular simulations but also for studies of liquid[47−57] and solid[58−66] systems.

Interfaces, as for example the contact between a solid and a liquid, are considered as one of the most intricate and challenging targets not only for experimentation but also for theoretical techniques. As mentioned QM studies have to employ simplified model systems of reduced size to keep the associated computing times within manageable bounds. The application of less time-consuming MM methods on the other hand suffers in many cases from a limited accuracy, being a consequence of the empirical nature of these approaches.

Since hybrid QM/MM techniques combine the advantages of QM and MM methodologies, they provide an adequate framework for the study of interface phenomena as well. As processes occurring at or near surfaces are linked to a large variety of problems in chemistry covering areas such as electrochemistry, corrosion, catalysis, and synthesis as well as biochemistry and material sciences, the availability of viable QM/MM simulation techniques enables theoretical studies of a broad range of chemical phenomena. This line of thought has already been followed in the embedded cluster approach,[58−63] in which the quantum mechanically treated region is surrounded by particles carrying effective potentials, representing the influence of the solid. If properly adjusted, the potential resulting from the embedding particles modulates the electron density thus mimicking the electronic structure in a solid. Without embedding electrons that should be subject to a bulk-like environment are exposed to a vacuum interface as well, which adversely influences surface properties. Embedding techniques thus provide an effective approach to balance accuracy of results with the associated computational effort. Although this setup enables investigations of various surface phenomena, typical implementations require some (if not all) of the embedding particles to remain at fixed positions. This, however, imposes restrictions on the system, making it unsuitable for all-atom structure predictions (i.e., only the positions of the so-called active atoms can be adjusted). Moreover, an application of an embedding setup relying on position restraints in the well-established molecular dynamics (MD) framework[67−70] describing the time-evolution of chemical systems is not possible: By ignoring forces acting on the restraint atoms, the sum of forces of the entire system does not equal zero. This violates Newton's third law of motion and thus the conservation of the overall linear momentum of the system. Further highly successful approaches for the treatment of solid-state surfaces are the QM/EFP and the SIMOMM methods,[71−80] the latter being an extension of the widely employed ONIOM approach.[81,82]

An alternative simulation strategy referred to as Car−Parrinello Molecular Dynamics (CPMD),[83−85] treating all particles of a system in the framework of Density Functional Theory[10,11] (DFT), is in principle well-suited to study surface phenomena. However, the number of atoms required to achieve an accurate representation of the system quickly becomes a limiting factor. Since the entire system is treated on a DFT basis, the possibility of vacuum artifacts as discussed above should also be taken into account when performing CPMD simulation of interfacial systems.

Thus, the aim of this work was to extend the capability and applicability of QM/MM simulation techniques to solid-state interfaces, thereby explicitly treating atoms of the solid quantum mechanically while not imposing any restraints to the atoms of the system. That way the QM/MM method can be combined with statistical simulation techniques such as molecule dynamics, which is expected to have a similar impact on surface chemistry and material sciences, as the combination of QM/MM approaches and the MD framework had on biochemistry and life sciences.

2. METHODOLOGY

2.1. Challenges for the QM/MM Treatment of a Solid-State Surface. A key element of hybrid simulation techniques is the separation of a chemical system into (at least) two zones: A smaller high-level region where the interactions are accounted for by accurate QM techniques and a low-level zone treating interactions via empirical MM models. However, after the respective atoms have been assigned to the QM zone, a simple-

DOI: 10.1021/acs.jctc.5b00548
J. Chem. Theory Comput. 2015, 11, 5873−5887

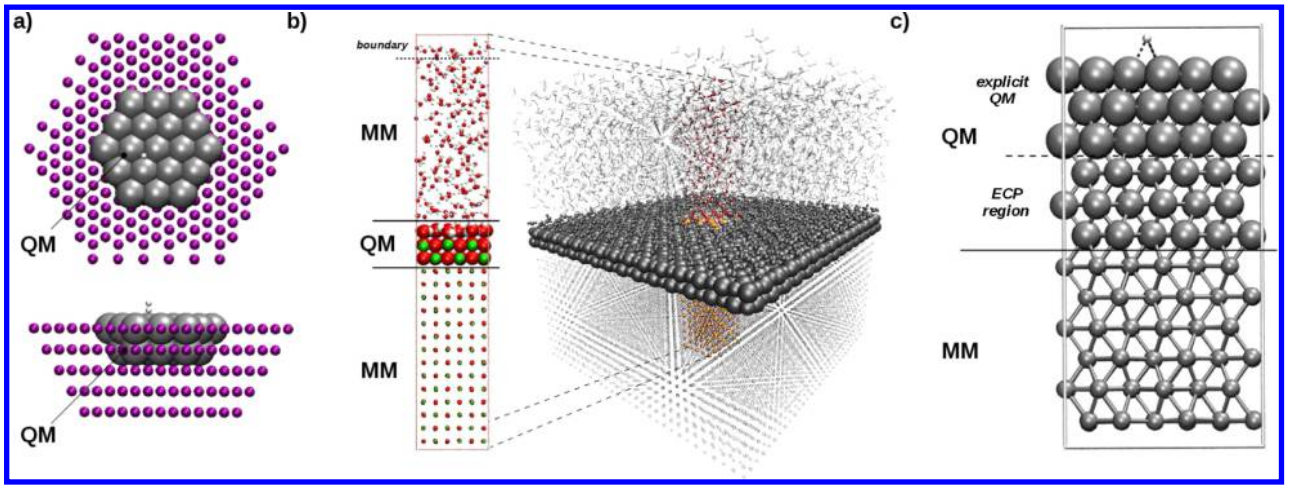

Figure 2. a) Exemplary setup of an embedded cluster setup for the study of hydrogen adsorption on a metallic surface. The quantum mechanically treated atoms are surrounded by embedding particles. In many cases only the substrate (H_2) is allowed to move, while the atoms of the surface remain fixed. b, c) Exemplary QM/MM setup for a MgO/water interface and hydrogen adsorption on a metallic beryllium surface. Employing a 2d quantum mechanical treatment and adequate QM-MM coupling potentials along with a suitable MM force field provides a suitable framework for all-atom structure optimizations as well as molecular dynamics simulation studies.

minded execution of the quantum mechanical computation would correspond to the treatment of the QM subsystem in vacuum, since all surrounding particles have been assigned to the MM region. Due to the mutual repulsion of electrons, the associated density tends to expand into the vacuum. However, this should only be the case for atoms close to the surface, while for all other atoms the density should approach that of the bulk. It can be expected that the electron density resulting from such an artificial *in vacuo* treatment is far from accurate, and as a consequence associated properties such as energies and forces acting on the nuclei show large deviations. For instance, if a large fraction of the electron density expands into the vacuum, the density in between the nuclei is lowered. Since the nuclei themselves experience a repulsive potential, the separation between layers of the solid increases which is demonstrated for an exemplary vacuum interface in the results section.

As mentioned, embedding techniques have proven as a simple yet effective measure to address this problem (cf. Figure 2a). In the case of ionic systems such as metal oxides the inclusion of the effective partial charges of the MM atoms close to the QM/MM boundary provides an adequate representation of the surrounding electrostatic potential. For example in the case of MgO values of $\pm 2.0e$ (e corresponding to the elementary charge) for Mg and O appear adequate,[86] although in some force field formulations the effective partial charges are chosen to be lower than the formal oxidation state (e.g., $\pm 1.14e$ for Zn and O in a novel potential model for ZnO[87]). All partial charges q of the M embedding atoms are included as an additional potential into the electronic Hamiltonian $\hat{H}_{el}$ of the n-electron QM system

$$\hat{H}_{el} = -\frac{1}{2}\sum_{i=1}^{n}\nabla_i^2 - \sum_{i=1}^{n}\sum_{J=1}^{N}\frac{Z_J}{\|\mathbf{r}_{ij}\|} + \sum_{i=1}^{n-1}\sum_{j=i+1}^{n}\frac{1}{\|\mathbf{r}_{ij}\|} - \sum_{i=1}^{n}\sum_{J=1}^{M}\frac{q_J}{\|\mathbf{r}_{ij}\|} \quad (1)$$

with N and Z being the number of nuclei and their associated charges, $\mathbf{r}$ representing a given distance vector, and the square of the del operator ∇ corresponding to the Laplacian. It can be seen that the final expression representing the influence of the point charges q is very similar to the electron-nuclei interaction, which both contribute to the comparably less demanding one-electron interactions. This technique often referred to as electrostatic embedding[44,88,89] provides a simple yet effective approach to account for an external charge distribution in the surrounding of the QM zone, while the associated increase in the computational effort remains moderate. Because only the electronic subsystem is treated quantum mechanically, interactions between nuclei are accounted for via a classical Coulomb potential. In the case of electrostatic embedding this applies also for the interactions between the MM partial charges.

For purely metallic systems the partial charges of (bulk) atoms are zero, and the embedding has to be performed via effective core potentials (ECPs, also referred to as pseudopotentials, PPs).[90−93] The initial idea of this approach is to represent a number of core electrons via an effective potential, since only valence electrons participate in the formation of chemical bonds. The respective Hamiltonian $\hat{H}_{ECP}$ is given as

$$\hat{H}_{ECP} = -\frac{1}{2}\sum_{i=1}^{n_v}\hat{\nabla}_i^2 + \sum_{i=1}^{n_v}\sum_{J=1}^{N}\left[V_J^{PP} - \frac{Z_J - n_J}{\|\mathbf{r}_{ij}\|}\right] + \sum_{i=1}^{n_v-1}\sum_{j=i+1}^{n_v}\frac{1}{\|\mathbf{r}_{ij}\|} \quad (2)$$

with n_v being the number of valence electrons (i.e., electrons treated explicitly), while n_J corresponds to the electrons of atom J represented by the one-electron pseudopotential operator V_J^{PP}. This potential ensures that the valence electrons remain outside the core region. In the case of an embedding procedure all-electron ECPs are assigned to the embedding atoms in the vicinity of the QM/MM interface to mimick the influence of the bulk on the QM region. To further improve the representation of the solid, the entire QM plus the ECP region may be further supported by layers of the solid treated via suitable MM potentials, using either pairwise force fields based on Lennard-Jones, Buckingham, or Morse formulations[13−15,94,95] or more sophisticated approaches such as shell-models[96] or many-body potentials.[97−99] Recently, general universal scaling formulations of the popular Mie, Lennard-Jones, Morse, and Buckingham

DOI: 10.1021/acs.jctc.5b00548
J. Chem. Theory Comput. 2015, 11, 5873−5887

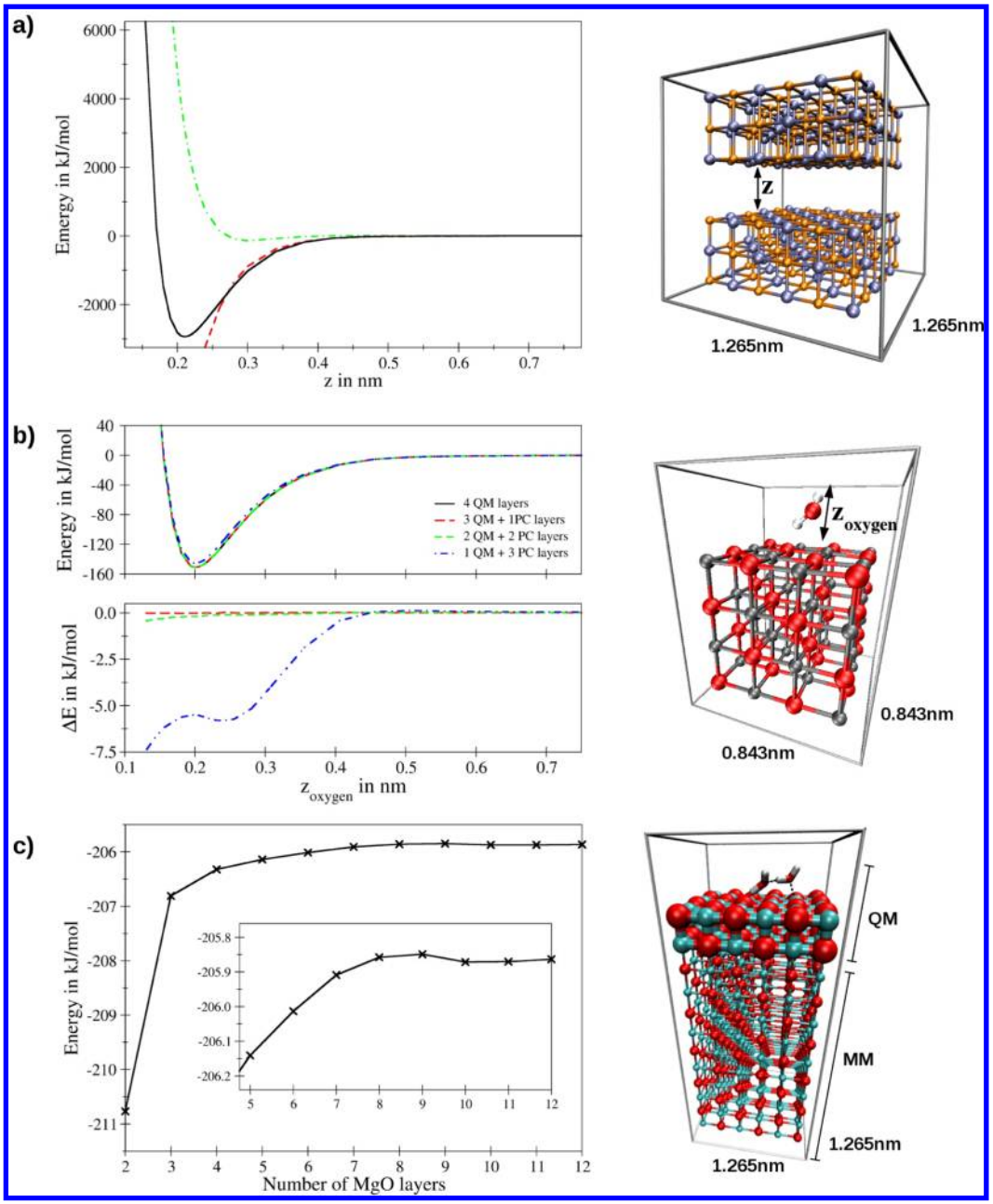

Figure 3. a) Potential energy scan obtained by moving three of the six MgO(100) layers along the *z*-axis. The black line is obtained from a full 2d-periodic QM treatment, while for the red curve the atoms of the three lowest layers are represented via MM partial charges (±2.0*e* for Mg and O). If properly adjusted non-Coulombic potentials (green) are provided, the full QM potential is accurately mimicked by the QM/MM treatment. b) Potential energy scans of a water binding the MgO(100) surface using different QM regions (top) and the associated energy difference to the full QM treatment (bottom). Inclusion of the first two layers of the solid into the QM region, while atoms in the lower layers are represented via MM partial charges (±2.0*e* for Mg and O) provides a very suitable compromise between effort and accuracy. c) Interaction energy of a water dimer adsorbed to the surface of MgO(100). A minimum of 2 QM and 8 MM layers is required to achieve convergence of the interaction energy (convergence criterion for optimization was set to $\leq 1.0 \times 10^{-4}$ kcal/mol Å).

potentials have been presented,[100−102] providing a sensible intermediate approach between the commonly used simple potentials and many-body potentials.

If the partial charges and all-electron ECPs are adequately parametrized, their potentials modulate the electron density in the quantum chemical treatment yielding a more appropriate representation of the system, while the computational cost is significantly lower compared to a full quantum treatment including all atoms in the QM zone. Although this technique provides an adequate representation of the QM system, interactions within the MM zone as well as the QM-MM coupling typically require the application of specifically adjusted interaction potentials.

For this reason the positions of selected embedding particles are in many cases chosen to be fixed, which implies that the forces acting on these atoms are neglected. As a consequence no structural relaxation of the embedding particles is possible, which may become a potential error source, especially for atoms close to the QM/MM boundary. As mentioned the sum of all remaining forces is not equal to zero, which violates Newton's

DOI: 10.1021/acs.jctc.5b00548
J. Chem. Theory Comput. 2015, 11, 5873−5887

third law of motion resulting in a change of the net linear momentum of the system. This is the reason why this type of embedding approach does not permit the application in the context of molecular dynamics simulations.[67−70]

However, even if adequate potential functions for the MM-MM and QM-MM interactions are provided the use of a finite-sized QM system may prove as a further error source. Such a setup may promote the occurrence of artificial shear-forces near the QM/MM boundary, leading to artificial repulsion or attraction between QM and MM subregions, i.e. the entire QM region is pulled to/pushed away from the embedding particle. Such a situation may be due to the fact that the QM-ECP interaction between particles of the surface can be expected to be different between the respective pairs in the bulk region (e.g., as it is the case the top and bottom layers of the QM region sketched in Figure 2a).

An excellent strategy to eliminate the possibility of such artifacts is to employ a 2d-periodic QM treatment, i.e. a slab-treatment as shown in the QM/MM setups presented in Figure 2b and c, in which entire layers of the solid are included into the QM region. Periodic quantum chemistry is based on the theorem derived by Felix Bloch[103] stating that the wave function of particles subject to a periodic potential $|\psi_{Bloch}\rangle$ consists of a periodic contribution $|\psi(\mathbf{r})\rangle$ modulated by a plane wave envelope function

$$|\psi_{Bloch}\rangle = |\psi(\mathbf{r})\rangle e^{i\mathbf{kr}} \tag{3}$$

with i being the imaginary unit, $\mathbf{r}$ is the particle position in the unit cell, and $\mathbf{k}$ is an associated wave vector. A linear combination of these so-called Bloch functions or, alternatively, the use of a plane wave basis enables a periodic quantum mechanical treatment of chemical systems in 1, 2, or 3 dimensions[84,104−109] implemented in a variety of QM packages such as Crystal,[110,111] VASP,[106,112] NWChem,[113] CPMD,[114] and CP2K,[115] typically in the context of density functional theory.

Considering the rapid decay of non-Coulombic interactions, their typical cutoff ranging from approximately 0.5 to 0.7 nm, the minimum size of the 2d-periodic unit cell for a QM/MM setup amounts to 1 nm × 1 nm. In the past the application of such a procedure to such a comparably large 2d-periodic supercell in the context of MD simulations requiring several hundreds to thousands of energy and force evaluations would have been a great challenge in terms of hardware resources (both in terms of memory as well as processing speed). However, the steady increase in the capacity of modern computational facilities does provide the required capacities to apply the outlined 2d-periodic QM/MM MD formulation, a trend that is expected to continue in the near future.

2.2. Feasibility of Placing the QM/MM Boundary within the Solid. A key question in formulating such a methodology is whether the concept of hybrid QM/MM methods can be extended to a 2d-periodic description of a solid system, which is discussed in the following in the case of exemplary metal oxide and metal surfaces. All computations have been performed with the Crystal09[110,111] suite at the DFT level using the Perdew-Burke-Enzerhofer functional.[116,117] The respective basis sets for H,[118] O,[119] Be,[120] and Mg[119] have been taken from the literature. The convergence criterion for the SCF procedure was set to 1.0×10^{-8} Hartree using the convergence aids according to the Broyden[121,122] and Anderson[123,124] schemes in the case of the metal oxide and metallic system, respectively. The respective cutoff radii have been set to half the lowest box dimension being 0.63 nm in the case of the metal oxide and 0.6 nm in the case of the metal system. Structure optimizations were performed until all force components were lower than 1.0×10^{-4} kcal/mol Å.

In order to compute the interaction energy E_{int} between two subsystems A and B, the respective energies E_A and E_B have been computed independently in the same periodic unit cell and subtracted from the associated total energy E_{AB}.

$$E_{int} = E_{AB} - E_A - E_B \tag{4}$$

This effectively resets the energy zero point to infinite z-separation between the 2d-periodic subsystems A and B.

2.2.1. MgO(100) Surface. Magnesium oxide, used as catalyst as well as support for high-temperature superconductors, is among the most widely investigated prototype systems to study surface properties and interfaces. Since reactions at mineral surfaces account for a large number of chemical reactions occurring in the Earth's crust, the simple rock salt-like structure of cubic MgO makes it an excellent target to study surface phenomena despite the rather low abundance of its naturally occurring mineral Periclase.[125]

MgO(100) is regarded as the thermodynamically most stable surface. Despite its apolar character it is known for its strong chemisorption of water molecules via partial dissociation.[126−128] The associated pH_{pzc} (point of zero charge) of 12.4 is among the highest reported values for mineral surfaces,[129] and numerous investigations highlight the very ordered hydration layers formed at the MgO−water interface.[125−136]

In order to assess whether the QM/MM framework can be extended to a periodic quantum chemical treatment, the interaction energy of a six-layer MgO model system with bulk-like spacing has been investigated as demonstrated in Figure 3a. By moving the lower three layers along the z-axis the respective energy as a function of distance was obtained (black line in Figure 3a). The resulting energy curve looks very similar to a typical binding interaction, but in this case it does not correspond to the interaction between two atoms but between entire layers of the solid. Replacement of all atoms in the lower slabs by point charges carrying $\pm 2.0e$ in the case of Mg and O corresponds to an electrostatic embedding treatment (red line in Figure 3a). It can be seen that at relatively short-range of approximately 0.4 nm the interaction energies obtained from the full-QM and the embedded-QM treatments coincide, indicating that only Coulombic interactions contribute to the total interaction beyond this distance. The difference between the full QM (black) and the QM-point charge (red) energy curves yields the non-Coulombic contributions to the interaction, which as expected are mainly required to represent the repulsive interaction at small layer separations. If appropriately adjusted non-Coulombic potentials (Mg_{QM}−Mg_{MM}, Mg_{QM}−O_{MM}, O_{QM}−Mg_{MM}, and O_{QM}−O_{MM}) are provided, the QM/MM interaction energy corresponds to that observed in the full QM treatment. In practice the non-Coulombic interactions between Mg and O atoms are the dominant contribution to the QM/MM coupling, and it was found that the same potential can be applied to the Mg_{QM}−O_{MM} and the O_{QM}−Mg_{MM} atom pairs. In addition this example clearly demonstrates that a non-Coulombic cutoff distance of 0.5 nm is indeed adequate.

To describe the MM-MM interaction a large number of suitable interaction potentials for virtually all types of chemical species are available in the literature. If all respective MM point charges are included into the QM calculation as an additional potential as given in eq 1, the associated MM-MM Coulombic contributions are included in the energy resulting from the QM

DOI: 10.1021/acs.jctc.5b00548
J. Chem. Theory Comput. 2015, 11, 5873−5887

calculation V_{QM}. Since the QM part accounts for periodicity in two dimensions, all MM-MM Coulombic interactions are also considered in a 2d-periodic framework, comparable to a 2d-Ewald summation.[137−140] Thus, electrostatic embedding has the additional benefit of outsourcing the demanding part of the MM-MM interaction to the parallelized and highly optimized routines of the QM program, provided that all MM atoms are included. At this point the only missing interactions are the non-Coulombic energy contributions between the MM atoms V_{MM}^{nC}, which are of short-ranged nature and are typically modeled via Lennard-Jones or similar formulations.

The associated contributions to the total Hamiltonian of the QM/MM system can thus be given as

$$H_{QM/MM} = \sum_{i=1}^{N+M} T_i + V_{QM} + \sum_{i=1}^{N}\sum_{j=1}^{M} V_{ij,QM/MM}^{nC} + \sum_{i=1}^{M-1}\sum_{j=i+1}^{M} V_{ij,MM}^{nC} \quad (5)$$

where N and M denote the number or particles in the QM and MM zone, T_i is the kinetic energy of the particle i, and V_{QM} is the energy obtained from the QM calculation. The contributions $V_{ij,QM/MM}^{nC}$ and $V_{ij,MM}^{nC}$ correspond to the non-Coulombic QM-MM and MM-MM interactions between particles i and j, respectively. Since the latter two interactions are fundamentally different, the application of separate non-Coulombic potentials proved necessary. In this work new parameters for the non-Coulombic QM-MM Lennard-Jones interaction have been derived based on the potential energy scan depicted in Figure 3a (see Supporting Information Figure S1). To describe the non-Coulombic interaction between MM particles the parameters reported by Long et al.[86] have been employed.

A further interesting detail in Figure 3a is the fact that although Coulombic interactions between two charges have a long-range character, the effective Coulombic interaction between the neutral slabs demonstrates a short-ranged nature, approaching zero already at 0.6 to 0.7 nm. This is in line with the basic concepts of the Wolf-summation technique,[141−143] which states that although the interaction between isolated point charges is long-ranged, the collective interaction between neutral clusters of atoms decays rapidly.

Figure 3b demonstrates that the use of two quantum mechanically treated layers plus two MM layers (representing the respective via point charges of ±2.0e for Mg and O, respectively) provides an adequate compromise between accuracy and computational effort to describe the H_2O/MgO(100) binding compared to a four-layer QM treatment of the system: After optimization of the orientation of a single water molecule on the surface, a potential energy scan with respect to the z-coordinate of the water molecule has been performed without changing its orientation. Next, the scan has been repeated successively replacing atoms in the lower layers with their associated partial charges.

When two QM and two MM layers are used the difference in energy with respect to the four-layer QM treatment at the minimum distance of ca. 0.21 nm is lower than 0.5 kJ/mol. In the case a more accurate estimation of the energy is required, three layers of the MgO surface can be included in the QM region, which essentially yields an identical binding compared to a four-layer QM treatment. It should be noted that in this computation non-Coulombic potentials between the water molecule and the MM atoms of the solid are not applied, since starting from the two-layer treatment the respective pair distances are beyond the typical non-Coulombic cutoff distances of approximately 0.5 to 0.7 nm. This explains why the one-layer QM treatment shows such a large deviation. However, a single QM layer cannot be expected to adequately reflect the electronic structure of a layered solid, and the use of only one layer can only be considered as a crude approximation even if the required non-Coulombic potentials were available.

With the finding that two layers provide an adequate compromise for the size of the QM region, it was of interest to investigate how many MM layers are required to converge the binding energy of adsorbed species. In order to investigate a more complex example of surface binding, a hydrogen bonded water dimer has been chosen as an example, and the respective binding energy obtained via unconstrained QM/MM energy minimization (i.e., all atoms of the system move according to the QM/MM potential) is shown in Figure 3c. The largest change in energy is observed when augmenting the two-layer QM treatment with a single layer of MM point charges, which highlights a key benefit of the QM/MM procedure: In the case of the two-layer QM treatment the entire system is exposed to the vacuum, enabling the electron density to expand into the vacuum on both sides of the system. This results in a stronger binding of an adsorbed species at the top layer, since a fraction of the density is exposed to the vacuum at the lower layer. Addition of further QM layers simply replicates the problem one layer at a time until a QM size is reached where the intermediate region of the solid shows bulk properties. However, the required system sizes to achieve such a convergence can be expected to push the computational effort beyond manageable bounds.

In the case of the embedded treatment (2 QM plus 1 MM layers), the electron density experiences a more adequate potential at the QM/MM interface and can only expand freely into the vacuum at the top layer. Since this leads to an increase of the surface density compared to the two-layer QM treatment, the binding energy is lowered by approximately 4 kJ/mol despite the larger number of interaction partners in the three-layer QM/MM treatment. Addition of more point charge layers to the MM zone further improves the modulation of the electron density; however, the change in energy is of smaller magnitude. Nevertheless, a total of 10 layers (2 QM plus 8 MM layers) is required to converge the binding energy of the water dimer at the surface. An all-atom quantum mechanical treatment of a 10-layer MgO(100) slab composed of 360 atoms is certainly at the limit of the capacities of modern computational facilities. As discussed in a 10-layer QM treatment the electron density in the lowest layers may again penetrate the vacuum, and it is questionable if a similar convergence behavior is observed when treating the systems only via QM. Even if a computational setup provides the resources to execute such computations, the proposed QM/MM framework requires only a fraction of the computing time, thus enabling for instance the execution of several investigations in parallel on high performance computing (HPC) facilities.

The performance of the 2d-periodic QM/MM setup is further demonstrated by comparing the average spacing of the minimum structures obtained from a six-layer full QM treatment with that of a 3 + 3 QM/MM setup shown in Figure S3. The individual layer separation agrees well with that obtained for the full QM treatment (deviation on the fourth significant digit) at significant lower computational cost. In particular the spacing between the first two layers is reproduced in excellent agreement with a deviation of 10^{-4} nm. Although a comparison with an even larger QM region composed of 10 or more layers would be highly

DOI: 10.1021/acs.jctc.5b00548
J. Chem. Theory Comput. 2015, 11, 5873−5887

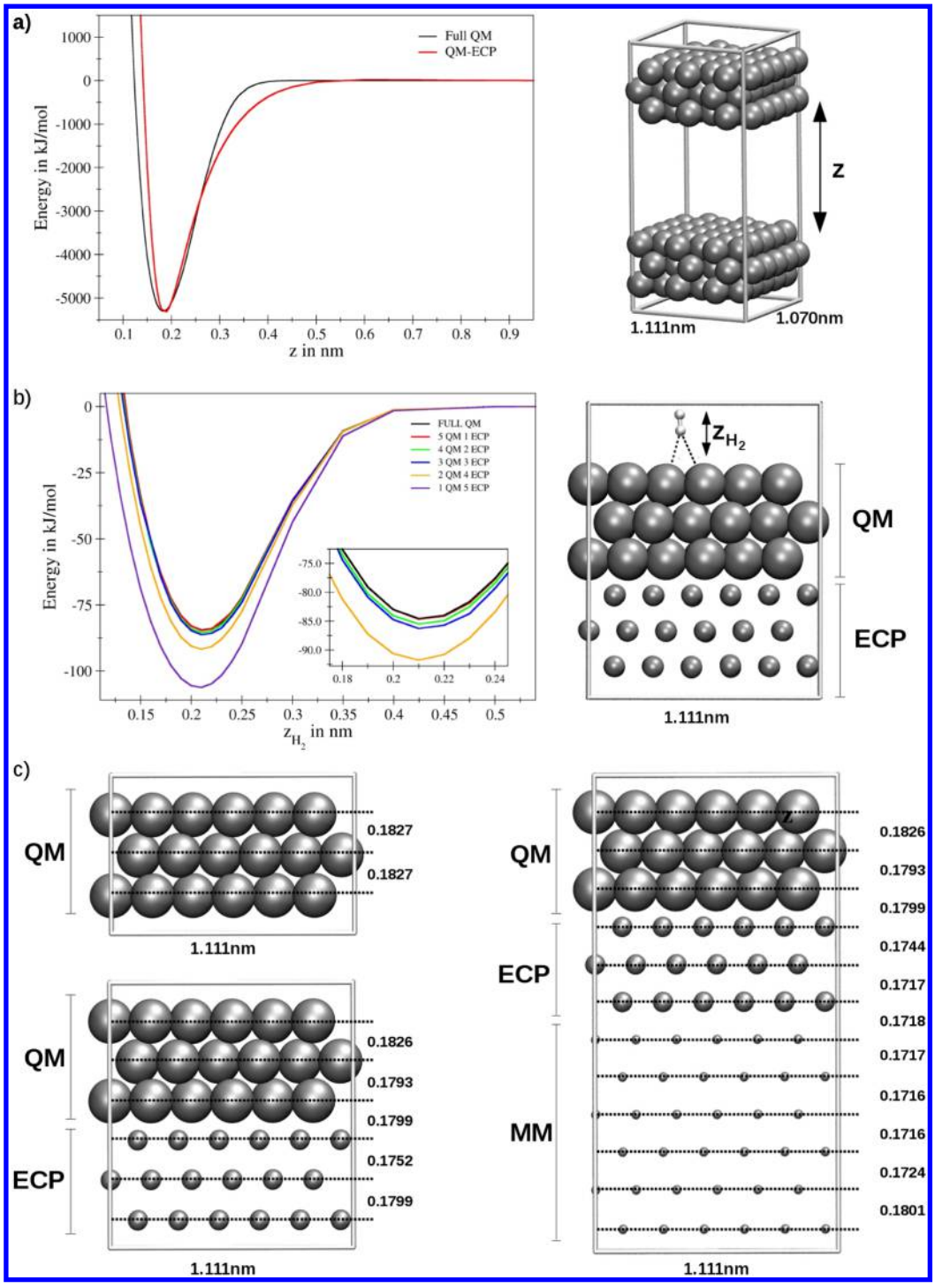

Figure 4. a) Potential energy scan moving three of the six Be(0001) layers along the *z*-axis. The black line results from a full 2d-periodic QM treatment, while for the red curve atoms in three lower layers are represented via all-atom ECPs. If these ECPs are properly adjusted, the interaction close to the minimum is adequately represented. No non-Coulombic QM-MM potentials are required. b) Potential energy scans of a hydrogen molecule binding to the Be(0001) surface using different QM/ECP setups. At least three layers of the solid have to be treated quantum mechanically. c) Minimum geometries and average layer separation $\langle z_i \rangle$ in nm for a QM, QM/ECP, and QM/ECP/MM setup. The representation of the bulk structure is dramatically improved in the latter case, which is expected to have a significant impact on processes occurring on the surface.

interesting, the available computational resources do not facilitate an increase of the system size. However, it can be expected that a similar agreement for the QM region will be observed.

2.2.2. Be(0001) Surface. Due to its low number of electrons and the closed-shell configuration of single Be atoms, Be(0001) proved as a suitable test system to investigate the application of a QM/MM framework in the case of a metal surface. Be surfaces are, however, not only interesting from the academic point of view. Owing to their favorable properties Be-lined surfaces are (along with tungsten applied to thermally critical areas) the preferred setup of the interior of experimental nuclear fusion reactors such as the Joint European Torus (JET) and the International Thermonuclear Experimental Reactor

DOI: 10.1021/acs.jctc.5b00548
J. Chem. Theory Comput. 2015, 11, 5873−5887

(ITER).[144−147] A beryllium atom may transform into tritium (^{3}H) upon impact with a neutron ejected during the fusion reaction.[148] Furthermore, beryllium has a high thermal conductivity, shows an absence of chemical sputtering, and is referred to as an excellent oxygen getter,[149,150] the latter being among the most potent plasma pollutants.

Similar as in the example of MgO present above a potential energy scan of the exemplary beryllium setup shown in Figure 4a was performed. Since in the case of metals atomic point charges are effectively zero, the embedding has to be carried out using properly adjusted all-electron ECPs (red line in Figure 4a). Considering that both helium and beryllium atoms contain only s-electrons, a helium core ECP proved as an adequate starting point to construct an embedding all-electron ECP for Be. By adjusting the respective parameters (see Supporting Information Table S1) reasonable agreement with a full-QM scan (black line in Figure 4a) is achieved. Although noticeable deviations can be observed, the minimum energy and the respective minimum distances are recovered with great accuracy. Since in an actual QM/MM study atoms near the QM/MM boundary should adapt the respective minimum configuration, the deviations at distances different from the minimum can be safely ignored. If it is required to mimic the full-QM scan with greater accuracy, additional functions could be employed when constructing the respective ECP. A particular advantage of specially adjusted ECPs is the fact that no further non-Coulombic potential for the QM-MM coupling is required, since minimum energy and distance are already recovered in the QM-ECP interaction.

Using quick test computations it is straightforward to show that there is zero interaction between two particles represented via all-electron ECPs, since they do not carry any electrons (data not shown). Thus, in order to describe the interaction between two such particles a classical potential is required, and a variety of suitable pairwise and many-body formulations for metallic systems are available in the literature. In this work a newly generated Morse potential has been constructed by fitting the QM-QM interaction shown in Figure 4a. A comparison of this fit is shown in the Supporting Information along with the respective potential parameters (see Figure S2).

Similar as in the case of the metal oxide surface it was of particular interest to investigate how many layers of the solid should be included in the QM region choosing molecular hydrogen as adsorbed species due to its closed shell configuration (cf. Figure 4b). The potential energy scan demonstrates that the binding energy of the H_2 molecule is very sensitive to the number of layers, with three QM layers plus three ECP layers marking the minimum size of the QM region, the respective deviation of energy being still approximately 2 kJ/mol. Addition of further ECP layers did not lead to any noticeable differences, however.

Considering structural arguments it is furthermore recommended to use an additional number of layers represented entirely via MM potentials below the QM/ECP region. Since these atoms are treated classically without assignment of an ECP, these layers are not visible to the QM treatment. The advantage of such a setup is demonstrated via the minimum structures shown in Figure 4c. The associated average layer separation $\Delta\langle z_{ij}\rangle$ is defined as

$$\Delta\langle z_{ij}\rangle = \langle z_i\rangle - \langle z_j\rangle \tag{6}$$

with $\langle z_i\rangle$ and $\langle z_j\rangle$ denoting the average z-coordinate of all atoms within layers i and j.

Energy minimization of just a three-layer QM system yields two identical values for $\Delta\langle z\rangle$ of 0.1827 nm resulting from the symmetry of the setup. Since the electron density expands into the vacuum in the top and bottom layers, a lower density is located in between the layers of the solid. That way the mutual repulsion between the nuclei is less shielded by the electrons, leading to an increased layer separation. This result demonstrates that a full-QM setup using just a few layers (i.e. a nanoslab) is not an ideal representation of a solid surface since the surface-to-bulk transition is not reflected in this setup.

Using the six-layer QM/ECP setup as shown in Figure 4c, the computational effort is only moderately increased, but the description of the solid surface is dramatically improved: Now the separation between the three QM layers is different, resulting from the influence of the embedding ECPs. A larger fraction of the electron density is now located in between the nuclei reducing the spacing between the individual layers. The separation between the vacuum exposed top layer and its first neighbor decreased to 0.1826 nm, and the average distance between the second and third layer shows a dramatic decrease to 0.1793 nm. Although the distance between the QM and ECP layers of 0.1799 is again slightly increased, the entire setup provides a much better representation of the bulk solid compared to the full-QM case, while the computational cost is still manageable. The final two values for $\Delta\langle z\rangle$ are mainly dominated by the properties of the applied MM model describing the interaction between the ECP particles. Since MM models also reflect the increase in separation near the vacuum border in an approximate way, a value of ca. 0.18 nm is observed between the lowest layers. This increase in separation can be expected to still have an undesired influence on processes occurring at the surface.

For this reason it is recommended to extend the computation to a QM/ECP/MM setup including a number of additional, purely MM-treated layers. While the additional computational effort is negligible, the increased separation of the bottom layers is shifted to the lowest slabs in the MM region and is, thus, not visible to the QM/ECP computation. All ECP layers resemble the bulk structure more closely, which is expected to improve the representation of the QM system even further. The use of a many-body potential such as a shell[96] or an embedded atom model[98] (EAM) may improve the description of the MM part beyond that of pairwise interactions. However, since the total separation between the top and bottom surface in this example is about 2 nm, the influence of the approximate treatment in the MM region can be expected to be safely ignored in most applications.

In addition, the inclusion of several layers of MM atoms is of further advantage for the application of the QM/MM procedure in molecular dynamics simulation studies. A low number of atoms typically results in large fluctuations in temperature and energy even if suitable thermostatization algorithms simulating the coupling with an external heat bath[67−70] are applied. The increased number of atoms in the QM/MM setup is thus beneficial for the thermalization of the system at negligible additional cost.

The total Hamiltonian for a system consisting of QM, ECP, and MM layers as shown in Figure 4c is then defined as

$$H_{\mathrm{QM/ECP/MM}} = \sum_{i=1}^{N+P+M} T_i + V_{\mathrm{QM}} + \sum_{i=1}^{M+P}\sum_{j=i+1}^{M+P} V_{ij,\mathrm{MM}} \tag{7}$$

with P being the number of atoms represented via all-electron ECPs. It was found that the application of the same potential

DOI: 10.1021/acs.jctc.5b00548
J. Chem. Theory Comput. 2015, 11, 5873−5887

$V_{ij,MM}$ for the ECP-ECP, ECP-MM, and MM-MM interaction leads to adequate results. It should be noted that for systems in which the QM-ECP contributions do not mimic the full-QM case as well as in this example (cf. Figure 6a), a further potential may be required to adjust the QM-ECP interactions. Similar as in the case of the non-Coulombic coupling in the MgO case, this correction potential can be expected to again require a different parameter set compared to the MM-MM interactions, requiring an additional potential contribution to eq 7.

Finally, the minimum structures predicted via a six-layer full QM treatment and a 3 + 3 QM/ECP setup have been compared as shown in Figure S4. Similar as in the case of MgO(001) the average distance between the first two layers is reproduced with high accuracy, the spacing in the bulk region agrees within $\leq 2.5 \times 10^{-3}$ nm, again at substantially reduced computational cost compared to the full QM treatment.

2.3. Molecular Dynamics Simulations. With the feasibility of the 2d-periodic QM/MM framework and its applicability in the context of energy minimization being outlined, two exemplary applications of this method in the context of molecular dynamics simulations are presented. The integration of the equation of motion has been carried out using the velocity Verlet algorithm[151,152] with a time-step of 0.2 fs corresponding to 5000 MD steps per picosecond. To model the influence of an external heat bath the Nose-Hoover chain thermostat[153−155] with a chain length of 5 has been employed. Data collection was performed every fifth MD step, i.e. one frame per femtosecond.

2.3.1. Water Adsorption at MgO(100). As discussed in the previous section a 10-layer setup (2 QM + 8 MM layers) was shown to be the minimum to converge the binding energy of an adsorbed water dimer. Although the computational cost is already significantly increased, an MD simulation study of the fully covered MgO(100) surface, i.e. a water monolayer at 100 K, was carried out. The low temperature was chosen to avoid evaporation of water molecules.

Figure 5a shows a snapshot of the simulation system. The 2d-periodic region depicted in color is treated as if it were surrounded by an infinite number of copies in the *x*- and *y*-directions, the first neighbor cells being depicted in gray. Figure 5b compares the in-plane distributions of water oxygen and hydrogen atoms with respect to the average z-coordinate of all atoms located in the first layer of the solid obtained from a 5 ps QM/MM MD simulation with data obtained from a classical MD simulation using the pairwise potentials reported by McCarthy et al.[156] Aside from notable deviations in peak height and position, the most striking difference is the absence of the peak at 0.1 nm in the plane-H distribution, clearly highlighting the missing surface protonation in the case of the classical simulation. Due to these proton transfer events hydroxide ions form in the solvent layer. Although the respective oxygen atoms appear at similar positions as those of adsorbed water molecules in the plane-O distribution (due to a similar O−O distance of the associated H-bonds), the orientation of the hydrogen atoms of hydroxide ions and water is different, which then leads to the observed double peaking in the plane-H distribution. Since using a nondissociative classical potential model in general prevents the occurrence of proton transfer events, only water molecules are observed in the monolayer. Thus, all hydrogen atoms are of similar type, which gives rise to a single peak in the plane-H distribution.

This example clearly demonstrates that the QM/MM treatment not only has the advantage of an accurate representation of the solid-ligand interaction at manageable computational cost discussed in the previous section. The

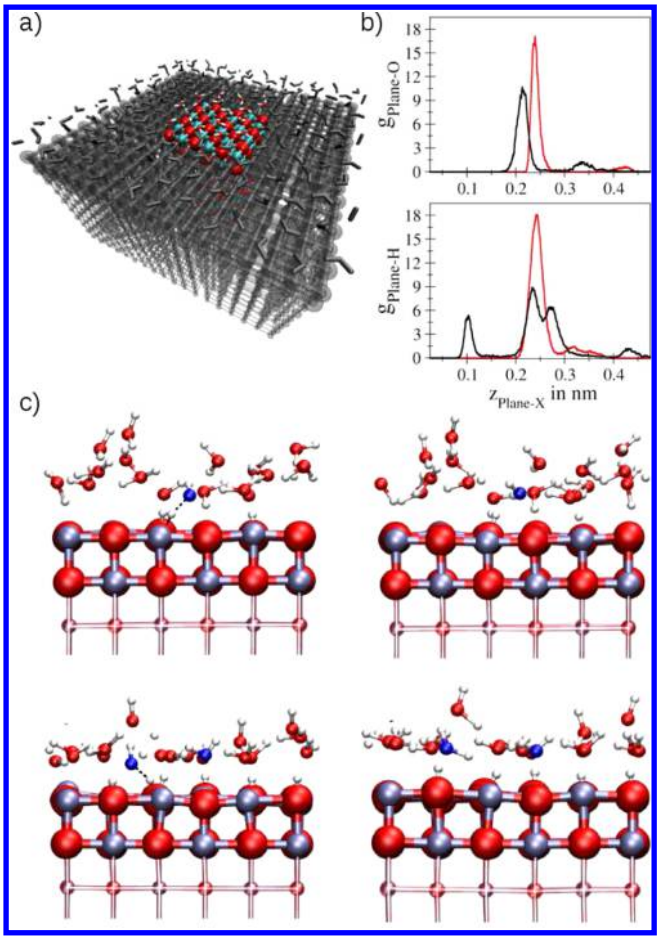

Figure 5. a) Setup of the MgO(100)/H_2O QM/MM system. The 2d-periodic region (colored) is treated as if it were surrounded by an infinite number of copies (first neighbor cells are depicted in gray). All water molecules plus the top two MgO layers are treated quantum mechanically. b) Pair distribution of water molecules with respect to the average $\langle z \rangle$ coordinate of all first layer atoms obtained from a QM/MM (black) and purely classical (red) description. The absence of the peak at 0.1 nm in the MgO−H distribution clearly demonstrates the missing surface protonation in the case of the classical setup. c) Snapshots obtained from the QM/MM simulation. Up to six oxygen atoms of the surface are found to be protonated in the various stages of the simulation. Due to the dynamical nature of the description, water molecules (marked in blue) are also reformed in the course of the simulation.

capability of describing the formation and cleavage of chemical bonds enables the study of successive protonation and deprotonation of oxygen atoms of the surface. Four selected snapshots of the MD simulation are depicted in Figure 5c. Up to six protonated surface oxygens have been registered along the simulation. This finding corresponds well to the discussion of Stumm stating that geometrical and chemical considerations indicate an average surface density of five (typically in the range of two to 12) hydroxyl groups per square nanometer of an oxide mineral.[129] Of course the protonation states are in constant equilibrium, leading to the reformation of water molecules thereby deprotonating the surface. The dynamics of these processes cannot be represented using a single (or few) minimum configuration obtained via energy minimization. According to statistical thermodynamics in such a case the properties of the system are governed by an ensemble, which can be probed by simulation methods such as Monte Carlo or, as in

DOI: 10.1021/acs.jctc.5b00548
J. Chem. Theory Comput. 2015, 11, 5873−5887

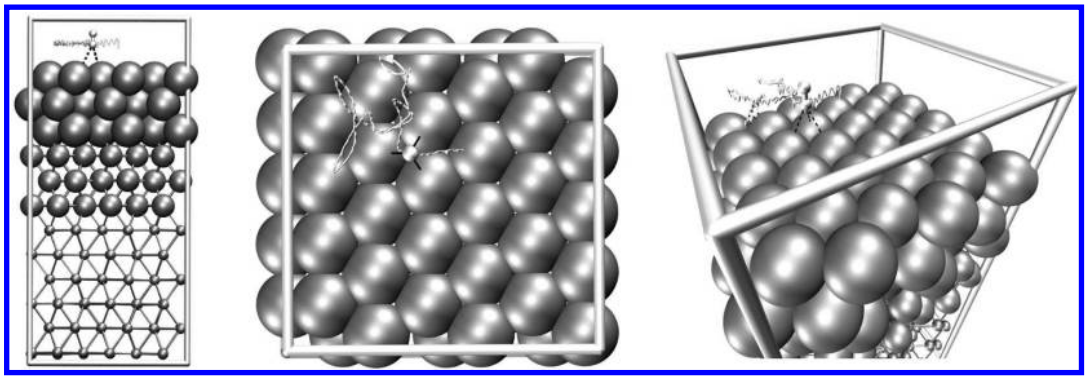

Figure 6. Front (left), top (center), and isometric (right) view of a selected configuration taken from a 5 ps exemplary QM/MM MD simulation of H_2 diffusion on Be(0001). The setup of the individual regions is according to Figure 4. The path marked in white depicts the trajectory of the center-of-mass of the H_2 molecule.

this case, molecular dynamics simulations.[67−70] In addition more elaborate schemes such as reaction path sampling[157,158] or advanced molecular dynamics approaches such as local elevation[122] or metadynamics[159] can be employed to probe individual reaction coordinates or accelarate the occurrence of rare events. Due to the required sampling of a large number of configurations in these approaches, the 2d-periodic QM/MM MD procedure outlined in this manuscript is of particular advantage to keep the associated computational effort manageable, while at the same time an increased accuracy of results is ensured.

An extension to include a further MM region on top of the water layer to model an actual solid−liquid interface is straightforward and has already been realized in the respective software. The associated computational effort resulting from the inclusion of another hundreds of partial charges leads to even longer computing times to achieve an acceptable trajectory length, and, therefore, the respective results have to be published at a later stage.

2.3.2. H_2 Adsorption on Be(0001). As discussed earlier beryllium is employed as lining material in experimental fusion reactors. A question that can be excellently addressed via simulation studies is the binding of small atomic and molecular species to the surface.

Figure 6 shows snapshots of a 5 ps MD simulation of H_2 to Be(0001) at 100 K employing the QM/ECP/MM setup depicted in Figure 4c, highlighting also the diffusion path of the molecule's center-of-mass. On average the distance to the surface of the two hydrogen atoms and the center of mass amounts to 0.212, 0.296, and 0.257 nm, respectively. Although as expected the diffusion path never leads on top of a Be atom, it changes direction multiple times thus forming a number of loops along the simulation. In order to demonstrate the diffusion path in more detail an animation of the simulation has been provided as a supplementary video. In addition to the concise depiction of the surface migration, this animation clearly demonstrates the advantage of the proposed QM/ECP/MM setup. All Be atoms are eligible to move independent of the assigned theoretical level. If the zone separation is not revealed the entire solid appears as a homogeneous unit.

The reason to select molecular hydrogen was its closed shell configuration making it a simpler target for an exemplary investigation. Although the computational effort for such a simulation is rather large, the proposed QM/ECP/MM setup can be employed to investigate the adsorption of other molecular species such as oxygen, nitrogen, and carbon dioxide as well as their atomic constituents. Furthermore, the setup can be extended to include surface motives such as steps, kinks, and defects in a straightforward way and, hence, provide a versatile and general framework to study surface phenomena. An extension of the setup to include a water monolayer as shown in the case of MgO(100) or even the inclusion of a further MM region to model a metal−water interface is readily implemented in the simulation software, its application only limited by the available computational infrastructure.

3. CONCLUSION AND OUTLOOK

The computational data presented in this article demonstrates that the principles of QM/MM calculations can be extended to a 2d-periodic quantum mechanical treatment of the high-level zone in a straightforward way. In both exemplary cases of a metal oxide as well as a metal surface it was shown that an embedding using atomic partial charges or all-atom ECPs can be employed to represent the potential energy scan of an associated full-QM treatment. In the case of metallic beryllium it was shown that no further classical potentials are required to adjust the QM/ECP interaction if the all-atom ECPs are properly adjusted. In the case of MgO(100) it could be shown that if adequate non-Coulombic potentials are provided, the full-QM treatment is accurately mimicked. In such a setup all particles are eligible to move according to the applied potential and the resulting forces, and no artificial position restraints are required. This makes the novel QM/MM framework applicable for all-atom structure optimizations (e.g., energy minimization, transition state, and reaction path optimization) as well as molecular dynamics simulations. Position restraints are a particularly profound obstacle in the latter case since the neglect of forces acting on the restraint particles results in a violation of momentum conservation.

Embedding has the advantage of modulating the electron density at the QM/MM interface within the solid, thus avoiding an expansion of the electron density into the vacuum. This not only influences the configuration of the solid (e.g., the layer separation in the case of Be) but also has a noticeable influence on the interaction of ligands bound to the surface. In order to converge these properties using a full-QM setup a large number of particles has to be included, greatly increasing resource requirements (memory and hard disk capacities) as well as the associated computing times. Moreover, in such a setup the lowest layer of the model is always exposed to the vacuum enabling the electron density to penetrate the vacuum. Thus, it can be expected that a full-QM treatment requires a larger number of layers to converge compared to a properly adjusted QM/MM

DOI: 10.1021/acs.jctc.5b00548
J. Chem. Theory Comput. 2015, 11, 5873−5887

setup. Furthermore, the presence of a rather large number of embedding and MM particles compared to QM nuclei is also of benefit for the thermalization of the system in MD simulations.

Despite the promising performance of the outlined QM/MM ansatz, the framework is also subject to a number of limitations. For instance each new solid system requires an elaborate setup procedure to provide especially adjusted QM/MM coupling potentials and/or all-atom ECPs. Test computations indicate that these potentials and ECPs show a rather large sensitivity to the basis and theoretical level employed in the full-QM references computation, the latter requiring a high computational demand. Further investigations using the QM/MM framework at different levels of theory and bases are required to assess the transferability of the coupling potentials and all-atom ECPs.

Due to the associated high computational effort the QM/MM framework is presently limited to density functional theory at the generalized gradient approximation (GGA) level.[10,11] This limitation can be overcome in the near future, however, since both hardware resources as well as software implementation are continuously improving. For instance due to the use of localized bases the crystal suite[110,111] is not only capable of computing exact exchange contributions enabling the application of Hybrid DFT methods. With the availability of a periodic Hartree−Fock framework post-HF methods such as periodic local Møller−Plesset perturbation theory of second order is already available in the CrysCorr program,[160] the only limiting factor being the available computational facilities. Considering the dramatic improvements achieved by formulating quantum mechanical algorithms in the context of linear scaling[161−163] and graphics processing units[164−169] (GPUs), present computational limitations can be expected to be overcome in the near future. Even then the availability of advanced QM/MM frameworks will be of interest to restrict the application of the QM routines to the chemical most relevant region enabling for instance the use of larger basis sets and/or larger unit cells.

The size of the unit cells used in this work of approximately 1 nm × 1 nm marks the lowest limit for the application of pairwise non-Coulombic potentials, requiring a minimum cutoff distance of 0.5 nm. Although it can be expected that the size of the unit cell will increase with the availability of improved computational resources and software, it will remain a limiting factor for future applications. In order to increase the unit cell by one or more orders of magnitude while at the same time still being able to describe the formation/cleavage of bonds, the application of reactive force field techniques is required. QM/MM frameworks such as the method outlined in this manuscript will provide a valuable source of data for the construction and assessment of reactive potential models. Established automated procedures to derive force field parameters from theoretical and/or experimental reference data[170,171] may greatly aid the construction of potentials from QM/MM data.

The data for MgO demonstrates that this compound is a particularly simple case of metal oxide. Comparing the Coulombic and non-Coulombic contributions of the 3 QM + 3 point charge layer scan depicted in Figure 3a is close to the results of the six-layer QM scan (black line). While the non-Coulombic contributions (green line) are important to represent the repulsion of the electrons at small layer separations, the attractive contributions are minor compared to the Coulombic part, amounting at most to 10−15% of the total interaction energy. Since this interaction is strongly dominated by the Coulombic contribution (i.e., an ionic character of the interaction), the covalency can be safely neglected. This situation will certainly change in the case of more complex oxides and related compounds such as metal sulfides, since the non-Coulombic character can be expected to be more significant. In this case frontier bonds treatable via capping techniques[172−175] or frontier orbital approaches[176−179] have to be applied if required. Recently, a detailed procedure to optimize link-atom parameters for different amino acids have been presented[180] which can also be applied in the case of the 2d periodic setup for oxide systems.

A particular challenge in the treatment of solid surfaces are polar surfaces showing a net dipole moment. Achieving an accurate description of such systems based on pairwise potentials is rather challenging, and more elaborate frameworks enabling a many-body description are required. Initial test computations have indicated that the QM/MM coupling potentials developed for MgO(100) can be applied without modification in the case of MgO(111), provided that all other settings associated with the QM computation (level of theory, basis sets, embedding procedure, ...) remain identical.

Despite these present limitations the outlined 2d-periodic QM/MM framework can be expected to provide a promising and versatile route for the investigation of a broad range of surface phenomena ranging from adsorption and catalysis to the treatment of more complex systems such as solid−liquid and solid−solid interfaces.

■ ASSOCIATED CONTENT

Supporting Information

The Supporting Information is available free of charge on the ACS Publications website at DOI: 10.1021/acs.jctc.5b00548.

Details about the fit of the MM pair potentials for MgO(001) and Be(0001) along with the respective parameters for the Morse potential used in the latter case, parameters of the Be all-electron ECP, and a comparison of the average layer spacing for optimized structures obtained via a six-layer full QM (left) and a 3 + 3 layer QM/MM setup of MgO(001) and QM/ECP for Be(0001) (PDF)

Short animation of the QM/ECP/MM simulation of H_2 on Be(0001) in mp4-format using VMD demonstrating the application of the QM/MM procedure in more detail[181] with video format supported in a variety of media players (for instance the free VLC media player, http://www.videolan.org/vlc/, available for a variety of operating systems) (MP4)

■ AUTHOR INFORMATION

Corresponding Author

*Phone: 43-512-507-57111. Fax: 43-512-507-57199. E-mail: T.Hofer@uibk.ac.at.

Notes

The authors declare no competing financial interest.

■ ACKNOWLEDGMENTS

Financial support for this work by a Ph.D. scholarship of the Leopold-Franzens-University of Innsbruck (Rector Prof. Dr.Dr.hc.mult. Tilmann Märk) for A.O.T. is gratefully acknowledged. This work was supported by the Austrian Ministry of Science BMWFW as part of the Konjunkturpaket II of the Focal Point Scientific Computing at the University of Innsbruck.

DOI: 10.1021/acs.jctc.5b00548
J. Chem. Theory Comput. 2015, 11, 5873−5887

REFERENCES

(1) Network, I. G. H. Milestones: Invention of the First Transistor at Bell Telephone Laboratories, Inc.; 2014.
(2) Nobel Prize in Chemistry 2013.
(3) Warshel, A.; Levitt, M. Theoretical Studies of Enzymic Reactions: Dielectric, Electrostatic and Steric Stabilization of the Carbenium Ion in the Reaction of Lysozyme. *J. Mol. Biol.* **1976**, *103*, 227.
(4) Aaqvist, J.; Warshel, A. Simulation of enzyme reactions using valence bond force fields and other hybrid quantum/classical approaches. *Chem. Rev.* **1993**, *93*, 2523.
(5) Field, M. J.; Bash, P. A.; Karplus, M. A Combined Quantum Mechanical and Molecular Mechanical Potential for Molecular Dynamics Simulations. *J. Comput. Chem.* **1990**, *11*, 700.
(6) Lyne, P. D.; Hodoscek, M.; Karplus, M. A hybrid QM-MM potential employing Hartree-Fock or density functional methods in the quantum region. *J. Phys. Chem. A* **1999**, *103*, 3462.
(7) Warshel, A. Molecular Dynamics Simulations of Biological Reactions. *Acc. Chem. Res.* **2002**, *35*, 385.
(8) Szabo, A.; Ostlund, N. S. *Modern Quantum Chemistry*; Dover Publications: New York, 1996.
(9) Helgaker, T.; Jørgensen, P.; Olsen, J. *Molecular Electronic Structure Theory*; Wiley: Chichester, 2000.
(10) Koch, W.; Holthausen, M. C. *A Chemist's Guide to Density Functional Theory*, 2nd ed.; Wiley-VCH: Weinheim, 2002.
(11) Sholl, D. S.; Steckel, J. A. *Density Functional Theory - a practical introduction*; Wiley: Hoboken, 2009.
(12) Schrödinger, E. Quantisierung als Eigenwertproblem (Vierte Mitteilung). *Ann. Phys.* **1926**, *386*, 109.
(13) Leach, A. R. *Molecular Modelling*; Prentice-Hall: Harlow, 2001; Vol. 2nd ed.
(14) Jensen, F. *Introduction to Computational Chemistry*; John Wiley & Sons Ltd.: Chichester, 2006; Vol. 2nd ed.
(15) Cramer, C. J. *Essentials of Computational Chemistry*; Wiley: West Sussex, 2002.
(16) Cygan, R. R.; Liang, J.; Kalinichev, A. G. Molecular Models of Hydroxide, Oxyhydroxide, and Clay Phases and the Development of a General Force Field. *J. Phys. Chem. B* **2004**, *108*, 1255.
(17) Maginn, E. J. Molecular simulation of ionic liquids: current status and future opportunities. *J. Phys.: Condens. Matter* **2009**, *21*, 373101.
(18) Borodin, O. Polarizable Force Field Development and Molecular Dynamics Simulations of Ionic Liquids. *J. Phys. Chem. B* **2009**, *113*, 11463.
(19) Dommert, F.; Wendler, K.; Berger, R.; Delle, S.; Holm, C. Force Fields for Studying the Structure and Dynamics of Ionic Liquids: A Critical Review of Recent Developments. *ChemPhysChem* **2012**, *13*, 1625.
(20) Jorgensen, W. L.; Tirado-Rives, J. The OPLS Force Field for Proteins. Energy Minimizations for Crystals of Cyclic Peptides and Crambin. *J. Am. Chem. Soc.* **1988**, *110*, 1657.
(21) Cornell, W. D.; Cieplak, P.; Bayly, C. I.; Gould, I. R.; Merz, K. M., Jr; Ferguson, D. M.; Spellmeyer, D. C.; Fox, T.; Caldwell, J. W.; Kollman, P. A. A Second Generation Force Field for the Simulation of Proteins, Nucleic Acids, and Organic Molecules. *J. Am. Chem. Soc.* **1995**, *117*, 5179.
(22) Jorgensen, W. L.; Maxwell, D. S.; Tirado-Rives, J. Development and Testing of the OPLS All-Atom Force Field on Conformational Energetics and Properties of Organic Liquids. *J. Am. Chem. Soc.* **1996**, *118*, 11225.
(23) MacKerell, A. D., Jr.; Banavali, N.; Foloppe, N. Development and current status of the CHARMM force field for nucleic acids. *Biopolymers* **2000**, *56*, 257.
(24) Duan, Y.; Wu, C.; Chowdhury, S.; Lee, M. C.; Xiong, G.; Zhang, W.; Yang, R.; Cieplak, P.; Luo, R.; Lee, T.; Caldwell, J.; Wang, J.; Kollman, P. A point-charge force field for molecular mechanics simulations of proteins based on condensed-phase quantum mechanical calculations. *J. Comput. Chem.* **2003**, *24*, 1999.
(25) Ponder, J. W.; Case, D. A. Force fields for protein simulations. *Adv. Protein Chem.* **2003**, *66*, 27.
(26) Mackerell, A. D. Empirical force fields for biological macromolecules: overview and issues. *J. Comput. Chem.* **2004**, *25*, 1584.
(27) Billeter, S. R.; van Gunsteren, W. F. A modular molecular dynamics/quantum dynamics program for non-adiabatic proton transfers in solution. *Comput. Phys. Commun.* **1997**, *107*, 61.
(28) Billeter, S. R.; van Gunsteren, W. F. Protonizable Water Model for Quantum Dynamical Simulations. *J. Phys. Chem. A* **1998**, *102*, 4669.
(29) Ojamäe, L.; Shavitt, I.; Singer, S. J. Potential models for simulations of the solvated proton in water. *J. Chem. Phys.* **1998**, *109*, 5547.
(30) van Duin, A. C. T.; Dasgupta, S.; Lorant, F.; Goddard, W. A. ReaxFF: A Reactive Force Field for Hydrocarbons. *J. Phys. Chem. A* **2001**, *105*, 9396.
(31) Liang, T.; Shin, Y. K.; Cheng, Y.; Yilmaz, D. E.; Vishnu, K. G.; Verners, O.; Zou, C.; Phillpot, S. R.; Sinnott, S. B.; van Duin, A. C. Reactive Potentials for Advanced Atomistic Simulations. *Annu. Rev. Mater. Res.* **2013**, *43*, 109.
(32) Hofmann, D. W. M.; Kuleshova, L.; D'Aguanno, B. A new reactive potential for the molecular dynamics simulation of liquid water. *Chem. Phys. Lett.* **2007**, *448*, 138.
(33) Buehler, M. J.; van Duin, A. C. T.; Goddard, W. A., III Multiparadigm Modeling of Dynamical Crack Propagation in Silicon Using a Reactive Force Field. *Phys. Rev. Lett.* **2006**, *96*, 095505.
(34) Mahadevan, T. S.; Garofalini, S. H. Dissociative Water Potential for Molecular Dynamics Simulations. *J. Phys. Chem. B* **2007**, *111*, 8919.
(35) Mahadevan, T. S.; Garofalini, S. H. Dissociative Chemisorption of Water onto Silica Surfaces and Formation of Hydronium Ions. *J. Phys. Chem. C* **2008**, *112*, 1507.
(36) Lammers, S.; Lutz, S.; Meuwly, M. Reactive force fields for proton transfer dynamics. *J. Comput. Chem.* **2008**, *29*, 1048.
(37) Webb, M. B.; Garofalini, S. H.; Scherer, G. W. Use of a Dissociative Potential to Simulate Hydration of Na^+ and Cl^- ions. *J. Phys. Chem. B* **2009**, *113*, 9886.
(38) Lee, S. H.; Rasaiah, J. C. Proton transfer an the mobilties of the H^+ and OH^- ions from studies of a dissociating model for water. *J. Chem. Phys.* **2011**, *135*, 124505.
(39) Hofer, T.; Hitzenberger, M.; Randolf, B. R. Combining a Dissociative Water Model with a Hybrid QM/MM Approach - A Simulation Strategy for the Study of Proton Transfer Reactions in Solutions. *J. Chem. Theory Comput.* **2012**, *8*, 3586.
(40) Wiedemair, M. J.; Hitzenberger, M.; Hofer, T. S. Tuning the reactivity of a dissociative force field: proton transfer properties of aqueous H_3O^+ and their dependence on the three-body interaction. *Phys. Chem. Chem. Phys.* **2015**, *17*, 10934.
(41) Wolf, M. G.; Groenhof, G. Explicit proton Transfer in Classical Molecular Dynamics Simualtions. *J. Comput. Chem.* **2014**, *35*, 657.
(42) Bakowies, D.; Thiel, W. *J. Phys. Chem.* **1996**, *100*, 10580.
(43) Gao, J. Potential of Mean Force for the Isomerization of DMF in Aqueous Solution: A Monte Carlo QM/MM Simulation Study. *J. Am. Chem. Soc.* **1993**, *115*, 2930.
(44) Lin, H.; Truhlar, D. G. QM/MM: what have we learned, where are we, and where do we go from here? *Theor. Chem. Acc.* **2007**, *117*, 185.
(45) Senn, H. M.; Thiel, W. QM/MM studies of enzymes. *Curr. Opin. Chem. Biol.* **2007**, *11*, 182.
(46) Metz, S.; Kästner, J.; Sokol, A. A.; Keal, T. W.; Sherwood, P. ChemShell - a modular software package for QM/MM simulations. *WIREs Comput. Mol. Sci.* **2014**, *4*, 101.
(47) Tuñón, I.; Martins-Costa, M. T. C.; Millot, C.; Ruiz-López, M. F. Coupled density functional/molecular mechanics Monte Carlo simulations of ions in water. The bromide ion. *Chem. Phys. Lett.* **1995**, *241*, 450.
(48) Staib, A.; Borgis, D. Molecular dynamics simulation of an excess charge in water using mobile Gaussian orbitals. *J. Chem. Phys.* **1995**, *103*, 2642.
(49) Tuñón, I.; Martins-Costa, M. T. C.; Millot, C.; Ruiz-López, M. F.; Rivail, J. L. A coupled density functional-molecular mechanics Monte Carlo simulation method: The water molecule in liquid water. *J. Comput. Chem.* **1996**, *17*, 19.

DOI: 10.1021/acs.jctc.5b00548
J. Chem. Theory Comput. 2015, 11, 5873−5887

(50) Gao, J. Hybrid Quantum and Molecular Mechanical Simulations: An Alternative Avenue to Solvent Effects in Organic Chemistry. *Acc. Chem. Res.* **1996**, *29*, 298.
(51) Rode, B. M.; Schwenk, C. F.; Hofer, T. S.; Randolf, B. R. Coordination and ligand exchange dynamics of solvated metal ions. *Coord. Chem. Rev.* **2005**, *249*, 2993.
(52) Rode, B. M.; Hofer, T. S.; Randolf, B. R.; Schwenk, C. F.; Xenides, D.; Vchirawongkwin, V. Ab initio Quantum Mechanical Charge Field (QMCF) Molecular Dynamics: A QM/MM - MD Procedure for Accurate Simulations of Ions and Complexes. *Theor. Chem. Acc.* **2006**, *115*, 77.
(53) Hofer, T. S.; Pribil, A. B.; Randolf, B. R.; Rode, B. M. Ab Initio Quantum Mechanical Charge Field Molecular Dynamics: A Non-parametrized First-Principle Approach to Liquids and Solutions. *Adv. Quantum Chem.* **2010**, *59*, 213.
(54) Hofer, T. S.; Rode, B. M.; Pribil, A. B.; Randolf, B. R. Simulations of Liquids and Solutions Based On Quantum Mechanical Forces. *Adv. Inorg. Chem.* **2010**, *62*, 143.
(55) Hofer, T. S.; Weiss, A. K. H.; Randolf, B. R.; Rode, B. M. Hydration of highly charged ions. *Chem. Phys. Lett.* **2011**, *512*, 139.
(56) Weiss, A. K.; Hofer, T. S. Exploiting the Capabilities of Quantum Chemical Simulations to Characterise the Hydration of Molecular Compounds. *RSC Adv.* **2013**, *3*, 1606.
(57) Hofer, T. S. Perspectives for hybrid ab initio/molecular mechanical simulations of solutions: from complex chemistry to proton-transfer reactions and interfaces. *Pure Appl. Chem.* **2014**, *86*, 105.
(58) Gonis, A.; Garland, J. W. Multishell method: Exact treatment of a cluster in an effective medium. *Phys. Rev. B* **1977**, *16*, 2424.
(59) Krüger, S.; Rösch, N. The moderately-large-embedded-clustermethod for metal surfaces; a density-functionalstudy of atomic adsorption. *J. Phys.: Condens. Matter* **1994**, *6*, 8149.
(60) Stefanovich, E. V.; Truong, T. N. Embedded density functional approach for calculations of adsorption on ionic crystals. *J. Chem. Phys.* **1996**, *104*, 2946.
(61) Jacob, T.; Fricke, B.; Anton, J.; Varga, S.; Bastug, T.; Fritzsche, S.; Sepp, W. Cluster-embedding method to simulate large cluster and surface problems. *Eur. Phys. J. D* **2001**, *16*, 257.
(62) Herschend, B.; Baudin, M.; Hermansson, K. A combined molecular dynamics+quantum mechanics method for investigation of dynamic effects on local surface structures. *J. Chem. Phys.* **2004**, *120*, 4939.
(63) Keal, T. W.; Sherwood, P.; Dutta, G.; Sokol, A. A.; Catlow, C. R. A. Characterization of hydrogen dissociation over aluminium-doped zinc oxide using an efficient massively parallel framework for QM/MM calculations. *Proc. R. Soc. London, Ser. A* **2011**, *467*, 1900.
(64) Bjornsson, R.; Bühl, M. Modeling Molecular Crystals by QM/MM: Self-Consistent Electrostatic Embedding for Geometry Optimizations and Molecular Property Calculations in the Solid. *J. Chem. Theory Comput.* **2012**, *8*, 498.
(65) Golze, D.; Iannuzzi, M.; Nguyen, M.; Passerone, D.; Hutter, J. Simulation of adsorption processes at metallic interfaces: An image charge-augmented QM/MM approach. *J. Chem. Theory Comput.* **2013**, *9*, 5086.
(66) Golze, D.; Hutter, J.; Iannuzzi, M. Simulation of adsorption processes at metallic interfaces: An image charge-augmented QM/MM approach. *Phys. Chem. Chem. Phys.* **2015**, *17*, 14307.
(67) Allen, M. P.; Tildesley, D. J. *Computer Simulation of Liquids*; Oxford Science Publications: Oxford, 1990.
(68) Sadus, R. J. *Molecular Simulation of Fluids: Theory, Algorithms, and Object-Orientation*; Elsevier: Amsterdam, 1999.
(69) Frenkel, D.; Smit, B. *Understanding Molecular Simulation*; Academic Press: San Diego − London, 2002.
(70) Tuckerman, M. E. *Statistical Mechanics: Theory and Molecular Simulation*; Oxford University Press: New York, 2010.
(71) Shoemaker, J. R.; Burggraf, L. W.; Gordon, M. S. SIMOMM: An Integrated Molecular Orbital/Molecular Mechanics Optimization Scheme for Surfaces. *J. Phys. Chem. A* **1999**, *103*, 3245−3251.
(72) Choi, C. H.; Gordon, M. S. Cycloaddition Reactions of 1,3-cyclohexadiene on the Silicon(001) Surface. *J. Am. Chem. Soc.* **1999**, *121*, 11311−11317.
(73) Shoemaker, J. R.; Burggraf, L. W.; Gordon, M. S. An Ab Initio Cluster Study of the Structure of the Si(001) Surface. *J. Chem. Phys.* **2000**, *112*, 2994−3005.
(74) Jung, Y.; Choi, C. H.; Gordon, M. S. Adsorption of Water on the Si(100) Surface: An Ab Initio and QM/MM Cluster Study. *J. Phys. Chem. B* **2001**, *105*, 4039−4044.
(75) Choi, C. H.; Liu, D.-J.; Evans, J. W.; Gordon, M. S. Passive and Active Oxidation of Si(100) by Atomic Oxygen: A Theoretical Study of Possible Reaction Mechanisms. *J. Am. Chem. Soc.* **2002**, *124*, 8730−8740.
(76) Choi, C. H.; Gordon, M. S. Cycloaddition Reactions of Acrylonitrile on the Si(100)-2 × 1 Surface. *J. Am. Chem. Soc.* **2002**, *124*, 6162−6167.
(77) Choi, C. H.; Gordon, M. S. *The Chemistry of Organic Silicon Compounds*; John Wiley & Sons, Ltd.: 2003; p 821.
(78) Ghosh, M. K.; Choi, C. H. Adsorption Reactions of Dimethylaluminum Isopropoxide and Water on the H/Si(100)-2 × 1 Surface:Initial Reactions for Atomic Layer Deposition of Al_2O_3. *J. Phys. Chem. B* **2006**, *110*, 11277−11283.
(79) Zorn, D. D.; Albao, M. A.; Evans, J. W.; Gordon, M. S. Binding and Diffusion of Al Adatoms and Dimers on the Si(100)-2 × 1 Reconstructed Surface: A Hybrid QM/MM Embedded Cluster Study. *J. Phys. Chem. C* **2009**, *113*, 7277−7289.
(80) Shoaib, M. A.; Choi, C. H. Adsorptions of HOCl on Ice Surface: Effects of Long-Range Electrostatics, Surface Heterogeneity, and Hydrogen Disorders of Ice Crystal. *J. Phys. Chem. C* **2012**, *116*, 3694.
(81) Svensson, M.; Humbel, S.; Froese, R. D. J.; Matsubara, T.; Sieber, S.; Morokuma, K. *J. Phys. Chem.* **1996**, *100*, 19357.
(82) Kerdcharoen, T.; Morokuma, K. ONIOM-XS: an extension of the ONIOM method for molecular simulation in condensed phase. *Chem. Phys. Lett.* **2002**, *355*, 257.
(83) Car, R.; Parrinello, M. Unified Approach for Molecular-Dynamics and Density Functional Theory. *Phys. Rev. Lett.* **1985**, *55*, 2471.
(84) Galli, G.; Parrinello, M. In *Computer Simulation in Materials Science*; Meyer, M., Pontikis, V., Eds.; Nato ASI Series E; Kluwer Academic: Dordrecht, Netherlands, 1991; Vol. *205*, Chapter 3.2, p 283.
(85) Kühne, T.; Krack, M.; Mohamed, F.; Parrinello, M. Efficient and Accurate Car-Parrinello-like Approach to Born-Oppenheimer Molecular Dynamics. *Phys. Rev. Lett.* **2007**, *98*, 066401.
(86) Long, Y.; Chen, N. X.; Wang, H. Y. Theoretical iinvestigations of misfit dislocations in Pd/MgO(001) interfaces. *J. Phys.: Condens. Matter* **2005**, *17*, 6149.
(87) Wang, S.; Fan, Z.; Koster, R. S.; Fang, C.; van Huis, M. A.; Yalcin, A. O.; Tichelaar, F. D.; Zandbergen, H. W.; Vlugt, T. J. H. New Ab Initio Based Pair Potential for Accurate Simulation of Phase Transitions in ZnO. *J. Phys. Chem. C* **2014**, *118*, 11050.
(88) Laio, A.; VandeVondele, J.; Rothlisberger, U. A Hamiltonian electrostatic coupling scheme for hybrid Car-Parrinello molecular dynamics simulations. *J. Chem. Phys.* **2002**, *116*, 6941.
(89) Voloshina, E.; Gaston, N.; Paulus, B. Embedding procedure for ab initio correlation calculations in group II metals. *J. Chem. Phys.* **2007**, *126*, 134115.
(90) Vanderbilt, D. Soft Self-Consistent Pseudopotentials in a Generalized Eigenvalue Formalism. *Phys. Rev. B: Condens. Matter Mater. Phys.* **1990**, *41*, 7892.
(91) Dagens, L. In *Computer Simulation in Materials Science*; Meyer, M., Pontikis, V., Eds.; Nato ASI Series E; Kluwer Academic: Dordrecht, Netherlands, 1991; Vol. *205*, Chapter 2.3, p 209.
(92) Schwerdtfeger, P. The Pseudopotential Approximation in Electronic Structure Theory. *ChemPhysChem* **2011**, *12*, 3143.
(93) Dolg, M.; Cao, X. Relativistic Pseudopotentials: Their Development and Scope of Applications. *Chem. Rev.* **2012**, *112*, 403.
(94) Harding, J. H. In *Computer Simulation in Materials Science*; Meyer, M., Pontikis, V., Eds.; Nato ASI Series E; Kluwer Academic: Dordrecht, Netherlands, 1991; Vol. *205*, Chapter 2.1, p 159.

DOI: 10.1021/acs.jctc.5b00548
J. Chem. Theory Comput. 2015, 11, 5873−5887

(95) Price, S. L. In *Computer Simulation in Materials Science*; Meyer, M., Pontikis, V., Eds.; Nato ASI Series E; Kluwer Academic: Dordrecht, Netherlands, 1991; Vol. *205*, Chapter 2.2, p 183.
(96) Dick, B. G., Jr.; Overhauser, A. W. Theory of the Dielectric Constants of Alkali Halide Crystals. *Phys. Rev.* **1958**, *112*, 90.
(97) Finnis, M. W.; Sinclair, J. E. A simple empirical N-body potential for transition metals. *Philos. Mag. A* **1984**, *50*, 45.
(98) Daw, M.; Baskes, M. Embedded-atom method: Derivation and application to impurities, surfaces, and other defects in metals. *Phys. Rev. B: Condens. Matter Mater. Phys.* **1984**, *29*, 6443.
(99) Stillinger, F. H.; Weber, T. A. Computer simulation of local order in condensed phases of silicon. *Phys. Rev. B: Condens. Matter Mater. Phys.* **1985**, *31*, 5262.
(100) Xantheas, S. S.; Werhahn, J. C. Universal scaling of potential energy functions describing intermolecular interactions. I. Foundations and scalable forms of new generalized Mie, Lennard-Jones, Morse, and Buckingham exponential-6 potentials. *J. Chem. Phys.* **2014**, *141*, 064117.
(101) Werhahn, J. C.; Akase, D.; Xantheas, S. S. Universal scaling of potential energy functions describing intermolecular interactions. II. The halide-water and alkali metal-water interactions. *J. Chem. Phys.* **2014**, *141*, 064118.
(102) Werhahn, J. C.; Miliordos, E.; Xantheas, S. S. A new variation of the Buckingham exponential-6 potential with a tunable, singularity-free short-range repulsion and an adjustable long-range attraction. *Chem. Phys. Lett.* **2015**, *619*, 133.
(103) Bloch, F. Über die Quantenmechanik der Elektronen in Kristallgittern. *Eur. Phys. J. A* **1929**, *52*, 555.
(104) Gillian, M. J. In *Computer Simulation in Materials Science*; Meyer, M., Pontikis, V., Eds.; Nato ASI Series E; Kluwer Academic: Dordrecht, Netherlands, 1991; Vol. *205*, Chapter 3.1, p 257.
(105) Blöchl, P. E. Projector augmented-wave method. *Phys. Rev. B: Condens. Matter Mater. Phys.* **1994**, *50*, 17953.
(106) Kresse, G.; Furthmüller, J. Efficiency of ab-initio total energy calculations for metals and semiconductors using a plane-wave basis set. *Comput. Mater. Sci.* **1996**, *6*, 15.
(107) Hill, J.; Subramanian, L.; Maiti, A. *Molecular Modeling Techniques in Material Science*; CRC Press: Boca Raton, 2005.
(108) Evarestov, R. A. *Quantum Chemistry of Solids*; Springer: Berlin, 2007.
(109) Anisimov, V.; Izyumov, Y. *Electronic Structure of Strongly Correlated Materials*; Springer: Berlin, 2010.
(110) Dovesi, R.; Orlando, R.; Civalleri, B.; Roetti, C.; Saunders, V. R.; Zicovich-Wilson, C. M. CRYSTAL: a computational tool for the ab initio study of the electronic properties of crystals. *Z. Kristallogr. - Cryst. Mater.* **2005**, *220*, 571.
(111) Dovesi, R.; Saunders, V. R.; Roetti, C.; Orlando, R.; Zicovich-Wilson, C. M.; Pascale, F.; Civalleri, B.; Doll, K.; Harrison, N. M.; Bush, I. J.; D'Arco, P.; Llunell, M. *CRYSTAL09 User's Manual*; University of Torino: Torino, 2009.
(112) Kresse, G.; Furthmüller, J. Efficient iterative schemes for ab initio total-energy calculations using a plane-wave basis set. *Phys. Rev. B: Condens. Matter Mater. Phys.* **1996**, *54*, 11169.
(113) Valiev, M.; Bylaska, E.; Govind, N.; Kowalski, K.; Straatsma, T.; Dam, H. V.; Wang, D.; Nieplocha, J.; Apra, E.; Windus, T.; de Jong, W. NWChem: A comprehensive and scalable open-source solution for large scale molecular simulations. *Comput. Phys. Commun.* **2010**, *181*, 1477–1489.
(114) CPMD, Copyright IBM Corp 1990–2008, Copyright MPI fr Festkrperforschung Stuttgart 1997–2001. http://www.cpmd.org/ (accessed Nov 1, 2015).
(115) VandeVondele, J.; Krack, M.; Mohamed, F.; Parrinello, M.; Chassaing, T.; Hutter, J. Quickstep: Fast and accurate density functional calculations using a mixed Gaussian and plane waves approach. *Comput. Phys. Commun.* **2005**, *167*, 103–128.
(116) Perdew, J. P.; Burke, K.; Ernzerhof, M. Generalized Gradient Approximation Made Simple. *Phys. Rev. Lett.* **1996**, *77*, 3865.
(117) Perdew, J. P.; Burke, K.; Ernzerhof, M. Generalized Gradient Approximation Made Simple (Errata). *Phys. Rev. Lett.* **1997**, *78*, 1396.
(118) Peintinger, M. F.; Oliveira, D. V.; Bredow, T. Consistent Gaussian basis sets of triple-zeta valence with polarization quality for solid-state calculations. *J. Comput. Chem.* **2013**, *34*, 451.
(119) Causà, M.; Dovesi, R.; Pisani, C.; Roetti, C. Electronic structure and stability of different crystal phases of magnesium oxide. *Phys. Rev. B: Condens. Matter Mater. Phys.* **1986**, *33*, 1308.
(120) Dovesi, R.; Pisani, C.; Ricca, F.; Roetti, C. Ab initio study of metallic beryllium. *Phys. Rev. B: Condens. Matter Mater. Phys.* **1982**, *25*, 3731.
(121) Broyden, C. G. A. Class of Methods for Solving Nonlinear Simultaneous Equations. *Math. Comput.* **1965**, *19*, 577.
(122) Johnson, D. D. Modified broyden's method for accelerating convergence in self-consistent calculations. *Phys. Rev. B: Condens. Matter Mater. Phys.* **1988**, *38*, 12807.
(123) Hamann, D. R. Semiconductor charge densities with hard-core and sofcore pseudopotentials. *Phys. Rev. Lett.* **1979**, *42*, 662.
(124) Anderson, D. G. Iterative Procedures for Nonlinear Integral Equations. *J. Assoc. Comput. Mach.* **1965**, *12*, 547.
(125) Refson, K.; Wogelius, R. A.; Fraser, D. G.; Payne, M. C.; Lee, M. H.; Milman, V. Water chemisorption and reconstruction of the MgO surface. *Phys. Rev. B: Condens. Matter Mater. Phys.* **1995**, *52*, 10823.
(126) Giordano, L.; Goniakowski, J.; Suzanne, J. Partial Dissociation of water molecules in the (3 × 2) Water Monolayer Deposited on the MgO(100) surface. *Phys. Rev. Lett.* **1998**, *81*, 1271–1273.
(127) Odelius, M. Mixed Molecular and Dissociative Water Adsorption on MgO(100). *Phys. Rev. Lett.* **1999**, *82*, 3919.
(128) Karalti, O.; Alfe, D.; Gillan, M. J.; Jordan, K. D. Adsorption of a water molecule on the MgO(100) surface as described by cluster and slab models. *Phys. Chem. Chem. Phys.* **2012**, *14*, 7846.
(129) Stumm, W. *Chemistry of the Solid-Water Interface*; John Wiley & Sons Ltd.: New York, 1992.
(130) Langel, W.; Parrinello, M. Hydrolysis at stepped MgO surfaces. *Phys. Rev. Lett.* **1994**, *73*, 504.
(131) Langel, W.; Parrinello, M. Ab initio molecular dynamics of H_2O adsorbed on solid MgO. *J. Chem. Phys.* **1995**, *103*, 3240.
(132) de Leeuw, N. H.; Parker, S. C. Molecular-Dynamics simulations of MgO surfaces in liquid water using a shell-model potential for water. *Phys. Rev. B: Condens. Matter Mater. Phys.* **1998**, *58*, 13901.
(133) Spagnoli, D.; Allen, J. P.; Parker, S. C. The Structure and Dynamics of Hydrated and Hydroxylated Magnesium Oxide Nanoparticles. *Langmuir* **2011**, *27*, 1821.
(134) Kamath, G.; Deshmukh, S. A.; Sankaranarayanan, S. K. R. S. Comparison of select polarizable and non-polarizable water models in prdicting solvation dynamics of water confined between MgO slabs. *J. Phys.: Condens. Matter* **2013**, *25*, 305003.
(135) Włodarczyk, R.; Sierka, M.; Kwapień, K.; Sauer, J. Structures of the Ordered Water Monolayer on MgO(001). *J. Phys. Chem. C* **2011**, *115*, 6764.
(136) Phan, A.; Ho, T. A.; Cole, D. R.; Striolo, A. Molecular Structure and Dynamics in Thin Water Films at Metal Oxide Surfaces: Magnesium, Aluminum, and Silicon Oxide Surfaces. *J. Phys. Chem. C* **2012**, *116*, 15962.
(137) Hockney, R. W.; Eastwood, J. W. *Computer Simulation Using Particles*; Taylor & Francis: New York, 1989.
(138) Solbrig, H. On the Ewald Summation Technique for 2D Lattices. *Phys. Status Solidi (a)* **1982**, *72*, 199.
(139) Yeh, I.; Berkowitz, M. L. Ewald summation for systems with slab geometry. *J. Chem. Phys.* **1999**, *111*, 3155.
(140) Grzybowski, A.; Gwóźdź, E.; Bródka, A. Ewald summation of electrostatic interactions in molecular dynamics of a three dimensional system with periodicity in two directions. *Phys. Rev. B: Condens. Matter Mater. Phys.* **2000**, *61*, 6706.
(141) Wolf, D. Reconstruction of NaCl surfaces from a dipolar solution to the Madelung problem. *Phys. Rev. Lett.* **1992**, *68*, 3315.
(142) Wolf, D.; Keblinski, P.; Phillpot, S. R.; Eggebrecht, J. Exact method for the simulation of Coulombic systems by spherically truncated, pairwise r^{-1} summation. *J. Chem. Phys.* **1999**, *110*, 8254.

DOI: 10.1021/acs.jctc.5b00548
J. Chem. Theory Comput. 2015, 11, 5873–5887

(143) Fennell, C. J.; Gezelter, J. D. Is the Ewald summation still necessary? Pairwise alternatives to the accepted standard for long-range electrostatics. *J. Chem. Phys.* **2006**, *124*, 234104.
(144) Batistoni, P.; Barbier, D.; Likonen, J. JET-EFDA Contributors, Fusion technology activities at JET in support of the ITER program. *Fusion Eng. Des.* **2013**, *88*, 733.
(145) Zalkind, S.; Polak, M.; Shamir, N. Effects of preadsorbed hydrogen on the adsorption of O_2, CO and H_2O on beryllium. *Surf. Sci.* **2003**, *539*, 81.
(146) Li, D.; Ouyang, Y.; Li, J.; Sun, Y.; Chen, L. Hydrogen storage of beryllium adsorbed on graphene doping with boron: First-principles calculations. *Solid State Commun.* **2012**, *152*, 422.
(147) Allouche, A. Quantum Modeling of Beryllium Surface Oxidation and Hydrogen Adsorption. *J. Phys. Chem. C* **2011**, *115*, 8233.
(148) Scaffidi-Argentina, F. Tritium and helium release from neutron irradiated beryllium pebbles from the EXOTIC-8 irradiation. *Fusion Eng. Des.* **2001**, *58*−*59*, 641.
(149) Tomastik, C.; Werner, W.; Störi, H. Oxidation of beryllium - a scanning Auger investigation. *Nucl. Fusion* **2005**, *45*, 1061.
(150) Philipps, V.; Mertens, P.; Matthews, G.; Maier, H.; JET-EFDA contributors. Overview of the JET ITER-like Wall Project. *Fusion Eng. Des.* **2010**, *85*, 1581.
(151) Verlet, L. Computer Experiments on Classical Fluids. I. Thermodynamical Properties of Lennard-Jones Molecules. *Phys. Rev.* **1967**, *159*, 98.
(152) Swope, W. C.; Andersen, H. C.; Berens, P. H.; Wilson, K. R. A computer simulation method for the calculation of equilibrium constants for the formation of physical clusters of molecules: Application to small water clusters. *J. Chem. Phys.* **1982**, *76*, 637.
(153) Hoover, W. G. Nonequilibrium Molecular Dynamics. *Annu. Rev. Phys. Chem.* **1983**, *34*, 103.
(154) Nose, S. A unified formulation of the constant temperature molecular-dynamics methods. *J. Chem. Phys.* **1984**, *81*, 511.
(155) Martyna, G. J.; Klein, M. L. Nose-Hoover chains: The canonical ensemble via continuos dynamics. *J. Chem. Phys.* **1992**, *97*, 2635−2645.
(156) McCarthy, M. I.; Schenter, G. K.; Scamehorn, C. A.; Nicholas, J. B. Structure and Dynamics of the Water/MgO Interface. *J. Phys. Chem.* **1996**, *100*, 16989.
(157) Bolhuis, P. G.; Chandler, D.; Dellago, C.; Geissler, P. L. TRANSITION PATH SAMPLING: Throwing Ropes Over Rough Mountain Passes, in the Dark. *Annu. Rev. Phys. Chem.* **2002**, *53*, 291.
(158) Wales, D. J. *Energy Lanscapes*; Cambridge University Press: Cambridge, 2003.
(159) Laio, A.; Parrinello, M. Escaping free-energy minima. *Proc. Natl. Acad. Sci. U. S. A.* **2002**, *99*, 12562.
(160) Pisani, C.; Maschio, L.; Casassa, S.; Halo, M.; Schütz, M.; Usvyat, D. Periodic Local MP2Method for the Study of Electronic Correlation in Crystals: Theory and Preliminary Applications. *J. Comput. Chem.* **2008**, *29*, 2113.
(161) Scuseria, E. G. Linear Scaling Density Functional Calculations with Gaussian Orbitals. *J. Phys. Chem. A* **1999**, *103*, 4782.
(162) Maurer, S. A.; Lambrecht, D. S.; Flaig, D.; Ochsenfeld, C. Distance-dependent Schwarz-based integral estimates for two-electron integrals: Reliable lightness vs. rigorous upper bounds. *J. Chem. Phys.* **2012**, *136*, 144107.
(163) Govoni, M.; Galli, G. Large Scale GW Calculations. *J. Chem. Theory Comput.* **2015**, *11*, 2680.
(164) Ufimtsev, I. S.; Martinez, T. J. Graphical Processing Units for Quantum Chemistry. *Comput. Sci. Eng.* **2008**, *10*, 26.
(165) Ufimtsev, I. S.; Martinez, T. J. Quantum Chemistry on Graphical Processing Units. 1. Strategies for Two-Electron Integral Evaluation. *J. Chem. Theory Comput.* **2008**, *4*, 222.
(166) Ufimtsev, I. S.; Martinez, T. J. Quantum Chemistry on Graphical Processing Units. 2. Direct Self-Consistent-Field Implementation. *J. Chem. Theory Comput.* **2009**, *5*, 1004.
(167) Ufimtsev, I. S.; Martinez, T. J. Quantum Chemistry on Graphical Processing Units. 3. Analytical Energy Gradients, Geometry Optimization, and First Principles Molecular Dynamics. *J. Chem. Theory Comput.* **2009**, *5*, 2619−2628.
(168) Watson, M.; Olivares-Amaya, R.; Edgar, R. G.; Aspuru-Guzik, A. Accelerating Correlated Quantum Chemistry Calculations Using Graphical Processing Units. *Comput. Sci. Eng.* **2010**, *12*, 40−51.
(169) Bao, J.; Feng, X.; Yu, J. GPU Triggered Revolution in Computational Chemistry. *Acta Phys.-Chim. Sin.* **2011**, *27*, 2019−2026.
(170) Grimme, S. A. General Quantum Mechanically Derived Force Field (QMDFF) for Molecules and Condensed Phase Simulations. *J. Chem. Theory Comput.* **2014**, *10*, 4497.
(171) Wang, L.; Martinez, T. J.; Pande, V. S. Building Force Fields: An Automatic, Systematic, and Reproducible Approach. *J. Phys. Chem. Lett.* **2014**, *5*, 1885.
(172) Amara, P.; Field, M. J. Evaluation of an ab initio quantum mechancial/molecular machanical hybrid-potential link-atom method. *Theor. Chem. Acc.* **2003**, *109*, 43.
(173) Field, M. J.; Bash, P. A.; Karplus, M. A combined quantum mechanical and molecular mechanical potential for molecular dynamics simulations. *J. Comput. Chem.* **1990**, *11*, 700.
(174) Zhang, Y.; Lee, T.; Yang, W. A pseudobond approach to combining quantum mechanical and molecular mechanical methods. *J. Chem. Phys.* **1999**, *110*, 46.
(175) Ihrig, A. C.; Schiffmann, C.; Sebastiani, D. Specific quantum mechanical/molecular mechanical capping-potentials for biomolecular functional groups. *J. Chem. Phys.* **2011**, *135*, 214107.
(176) Théry, V.; Rinaldi, D.; Rivail, J.; Maigret, B.; Ferenczy, G. G. Quantum mechanical computations on very large molecular systems: The local self-consistent field method. *J. Comput. Chem.* **1994**, *15*, 269.
(177) Assfeld, X.; Rivail, J. Quantum chemical computations on parts of large molecules: the ab initio local self consistent field method. *Chem. Phys. Lett.* **1996**, *263*, 100.
(178) Gao, J.; Amara, P.; Alhambra, C.; Field, M. J. A generalized hybrid orbital (GHO) method for the treatment of boundary atoms in combined QM/MM calculations. *J. Phys. Chem. A* **1998**, *102*, 4714−4721.
(179) Philipp, D.; Friesner, R. A. Mixed ab initio QM/MM modeling using frozen orbitals and tests with alanine dipeptide and tetrapeptide. *J. Comput. Chem.* **1999**, *20*, 1468.
(180) Hitzenberger, M.; Hofer, T. S. Probing the range of applicability of structure- and energy-adjusted QM/MM link bonds. *J. Comput. Chem.* **2015**, *36*, 1929.
(181) Humphrey, W.; Dalke, A.; Schulten, K. VMD - Visual Molecular Dynamics. *J. Mol. Graphics* **1996**, *14*, 33−38.

DOI: 10.1021/acs.jctc.5b00548
J. Chem. Theory Comput. 2015, 11, 5873−5887